DOI 10.1007/s11204-021-09728-w
Soil Mechanics and Foundation Engineering, Vol. 58, No. 3, July, 2021 (Russian Original No. 3, May-June, 2021)

SOIL MECHANICS

EVOLUTION OF THE PORE CHARACTERISTICS OF RED CLAY UNDER AXIAL STRAIN

UDC 624.131.439.3

Lijie Chen,[1] Xuejun Chen,[1*] and He Wang[2]
[1]College of Civil and Architecture Engineering, Guilin University of Technology, Guilin 541004, China; [2]Army Engineering University, Nanjing 210007, China, Corresponding author Email: xuejunchen@126.com.

To study the evolution of pore structure in red clay during triaxial shear, nuclear magnetic resonance tests were performed on soil samples to determine their pore characteristics after undergoing different shear strains during triaxial consolidated undrained shear tests under different confining pressures. The results showed that the effects of confining pressure and shear on the intragranular pores of the soil samples were minimal. In contrast, during consolidation and triaxial shear, interparticle macropores in the soil sample were compressed. Generally, the greater the confining pressure during the test, the faster the soil structure stabilized. Once the axial strain exceeded 8%, the soil structure also stabilized, and both deviatoric stress and pore diameter remained unchanged. Evolution of the pore characteristics during triaxial shear revealed that their shear deformation history determined the new microstructure of the saturated compacted red clay.

Introduction

The microscopic structure of the soil is an important factor affecting engineering properties, like soil strength and permeability [1]. Since Terzaghi (1925) presented the first structural concept of soil, many scholars have carried out research based on this concept. When the microstructure of the soil changes, the pore distribution can change markedly, allowing variation of soil structure to indicate changes in pore distribution [2-4]. Alonso et al. measured the porosity of compacted soil by mercury intrusion porosimetry and quantified soil microstructures under wet and dry conditions [5]. Lin et al. studied the microscopic properties of bentonite using scanning electron microscopy and explained its macroscopic mechanical behavior with reference to its microscopic properties [6]. Tao et al. used ANSYS software (ANYS, Inc., Canonsburg, PA, USA) to establish a microscopic model of clay to analyze the influence of confining pressure related to consolidation on soil stress and microscopic deformation; they quantified the evolution of pore size using Image-Pro Plus software [7]. These studies used mercury intrusion tests and scanning electron microscopy to analyze soil pore structure characteristics. Both methods require drying of the soil sample, which is not ideal given that drying is complicated, time-consuming, and may affect the soil sample's pore structure.

In recent years, nuclear magnetic resonance (NMR) has been widely used to study the microstructures of rocks and soils because of its many advantages, including being time-saving, nondestructive, and sensitive to hydrogen-containing fluids [8-10]. Zhou et al. used a rock mechanics apparatus to perform different degrees of axial compression on marble and used NMR to evaluate porosity changes and determine the evolution of porosity during failure [11]. Liu et al. conducted a true triaxial

Translated from Osnovaniya, Fundamenty i Mekhanika Gruntov, No. 3, p. 10, May-June, 2021.
0038-0741/21/5803-0196 ©2021 Springer Science+Business Media, LLC

TABLE 1

Sample No.	Test confining pressure (kPa)	Triaxial shear axial strain (%)	Shearing Stage
1-1	100	0	0
1-2	100	8	I
1-3	100	16	II
1-4	100	24	III
2-1	200	0	0
2-2	200	8	I
2-3	200	16	II
2-4	200	24	III
4-1	400	0	0
4-2	400	8	I
4-3	400	16	II
4-4	400	24	III

consolidation undrained shear test on undisturbed silty soil and analyzed the influence of the shear rate and shear degree on the microscopic porosity of this soft soil using NMR [12]. They also used NMR to analyze the effects of axial strain changes on the pore structure of rock and undisturbed soil in triaxial shear tests. To date, few studies have analyzed the porosity changes of compacted red clay during triaxial shearing. To study the influence of confining pressure and axial strain on the microstructure of remolded red clay, we used NMR to quantify the pore distribution and determine the influence of confining pressure and shear on the evolution of the pore size distribution.

Materials and Methods

The red clay used in this study was obtained from a 5 m depth near Guilin, Guangxi Province, China. The red clay was air-dried and crushed to screen soil particles, yielding particle sizes of less than 2 mm for testing. The red clay has a specific gravity of 2.75, a liquid limited water content of 59.5%, a plastic limit moisture content of 37%, a plasticity index of 22.5%, a maximum dry density of 1.67 g/cm^3, and an optimum moisture content of 31%.

Red clay having a water content of 31% was pressed into a cylindrical-shaped sample, having a height of 80 mm, a diameter of 39.1 mm, and a dry density of 1.40 g/cm^3. The triaxial tests on these samples had a saturation of 98% and involved consolidation under three confining pressures (100, 200, and 400 kPa). When the soil consolidation degree reached 95%, the soil samples were deformed at a shear rate of 0.08 mm/min. We used a TKA-TTS1 triaxial instrument, produced by Nanjing TKA Technology Co., Ltd. (China).

The triaxial sheared sample was analyzed using a MacroMR12 nuclear magnetic resonance instrument manufactured by Suzhou Niumag Analytical Instruments Co., Ltd. (China). The test magnet probe was a MacroMR12-110H-I-60mm-plus. The test parameters were set as follows: The Carr-Purcells Meiboom Gill spin echo (CPMG) for pulse sequence had an echo time of 0.5 ms and a repetition time of 1000 ms; 1000 echoes were used to obtain the free induction decays (FID) curve of water for all samples with a scan number (NS) of 16. The sample numbers and test control conditions of this study are listed in Table 1.

Test Results and Discussion

Pore number and pore size changes

The transverse surface relaxation time (T_2) curves measured by NMR of soil samples after triaxial shear under different experimental conditions are shown in Fig.1. These curves reflect the pore number and pore size of the soil samples.

The pore size is positively correlated with the T_2 value. Generally, the relaxation time increases as pore size in the soil sample increases. The area below the T_2 curve represents the porosity of the sample. The larger the peak area, the larger the pore content in the corresponding pore size range. Most

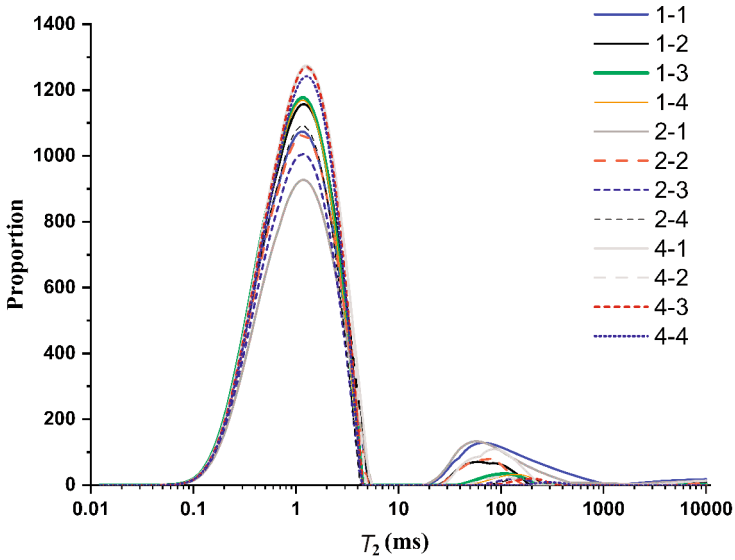

Fig. 1. Transverse surface relaxation time (T_2) curves of red clay samples (see legend) under different experimental conditions (listed in Table 1).

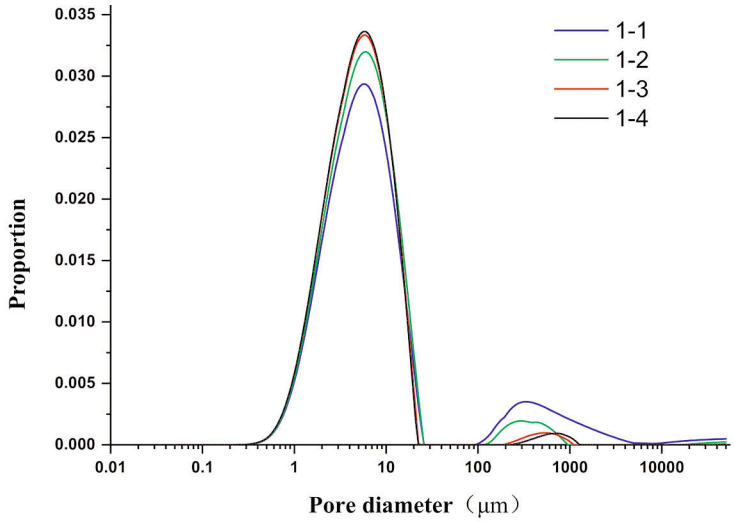

Fig. 2. The pore diameter curves of red clay samples (see legend) under different test conditions (listed in Table 1).

T_2 curves had two peaks, although some had a third peak. There were clear boundaries between peaks.

The pore diameters of the sample can be obtained from the T_2 curve:

$$r_c = T_2 \rho_2 F_s, \tag{1}$$

where r_c is the radius of the pores, ρ_2 is the surface relaxivity, and F_s is the pore shape influence factor (F_s = 3 for a spherical shape and F_s = 2 for a cylindrical shape). In this study, the pore shape was assumed to be spherical (F_s = 3).

The relaxation time varied linearly with pore radius, causing pore distribution of the red clay to reflect relaxation time T_2. All curve shapes were similar. The pore diameter distributions of soil samples at increments of 0%, 8%, 16%, and 24% of axial strain at a confining pressure of 100 kPa are shown in Fig. 2. The pores of the soil samples had a bimodal distribution, with peaks representing micropores and macropores of the sample. The content of the micropores was much higher than that of the macropores.

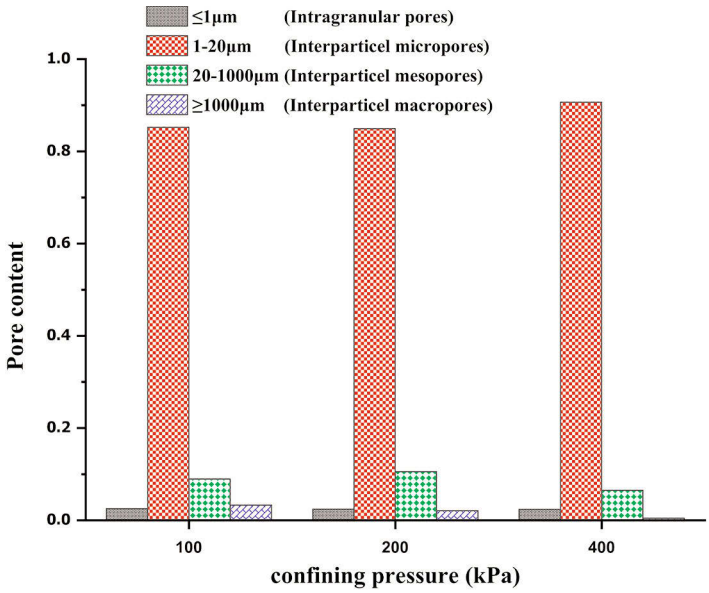

Fig. 3. The pore distributions of soil samples consolidated under different confining conditions.

The pore radius of the macropores was between 100 and 10,000 μm, and the pore radius of the micropores was between 0.1 and 50 μm.

Herein, deformation stages were defined according to degree of strain, referred to as Stage I (0%-8% strain), Stage II (8%-16% strain), and Stage III (up to 24% strain). During Stage I, the amplitude of the micropore distribution curve increased, although the pore size distribution interval did not change. The peak of the pore size distribution curve of the macropores moved to the right, while the peak area decreased, causing the pore size distribution interval to narrow. Therefore, when the axial strain was less than 8%, the number of pores with a pore diameter of 100-10,000 μm in the soil sample decreased, while those with a pore diameter of more than 10,000 μm disappeared. In contrast, the number of pores with a pore diameter of 0.1-50 μm increased.

In Stage II, the increase in micropore content was much slower than during Stage I. Meanwhile the distribution interval of macropores continued to decrease, with the peak moving further to the right, as peak area decreased markedly. This indicates that as axial strain increased, the macropores of the soil sample were compressed to a lesser extent. There was little change between the pore distributions of Stages II and III, indicating that the internal structure of the soil sample stabilized once axial strain exceeded 16%.

Pore distribution changes

The pore distribution of soil samples consolidated under the constraints of 100, 200, and 400 kPa are shown in Fig. 3. Generally, consolidation had little effect on intragranular pore contents. Delage and Lefebvre showed that the pores within soil particles do not break during remodeling because of strong cementation [3]. In this study, under low confining pressures (100, 200 kPa), the intragranular pore content of soil particles did not change noticeably. When the confining pressure increased to 400 kPa, the pore volume increased by 6.8% compared to pore volumes under 100 and 200 kPa. Although the interparticle mesopores consolidated under low confining pressures (100 and 200 kPa), the pore content changed little. When the confining pressure was higher (400 kPa), the interparticle mesopores were reduced by 27.1% compared with the pore volume under a confining pressure of 100 kPa, while inter-

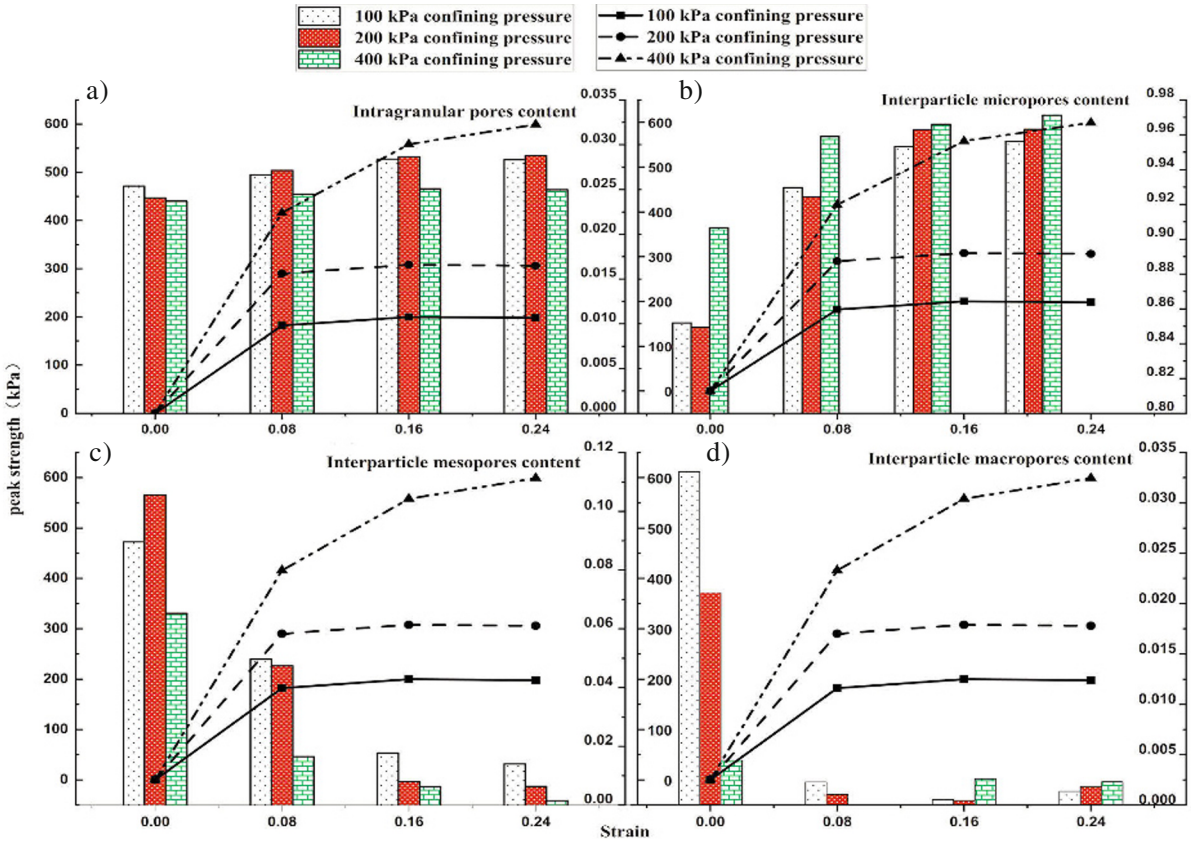

Fig. 4. Evolution of the deviatoric stress peak and pore distribution under different axial strains: a) intragranular pores; b) interparticle micropores; c) interparticle mesopores; d) interparticle macropores.

particle mesopore content between particles was reduced by 38.2% compared to that under a confining pressure of 200 kPa. Clearly, interparticle macropore contents decreased markedly as the confining pressure increased.

During consolidation, the stress state of the soil changed as the volume of the soil was gradually compressed, and some of the pore water was discharged from the soil sample. The soil skeleton became the main supporting structure of the applied force. At the confining pressure of 100 kPa, there was only a slight compression effect on the interparticle macropores. As confining pressure increased, the interparticle mesopores began to compress. During the consolidation of red clay soil samples, the interparticle macropores compressed first. Once the confining pressure increased to 200 kPa, the interparticle macropores were compressed, while the content of interparticle mesopores increased. Once the confining pressure increased to 400 kPa, most of the interparticle macropores and some of the interparticle mesopores compressed into interparticle micropores, causing the interparticle micropore content of the soil sample to increase.

Changes under triaxial shear

The pore distributions of triaxial sheared soil samples under different confining conditions (100, 200, and 400 kPa) and different axial strains (0%, 8%, 16%, and 24%) are shown in Fig. 4.

The pore radius distributions of soil samples under different conditions were similar. Typically, as confining pressure and axial strain increased, the intragranular pores changed little, indicating that the confining pressure and compression shearing had little effect on intragranular pores.

During Stage I, as the axial strain increased, the deviatoric stress of the soil sample increased rapidly, and the content of interparticle micropores changed markedly. When the axial strain was less than 8%, triaxial shearing had a major effect on the structure of the soil samples. Under a confining pressure of 400 kPa, the variation ranges of the three kinds of pores (interparticle micropores, mesopores, and macropores) were larger than those under 100 and 200 kPa confining pressures. During the test, the pore structure of the soil underwent a rapid adjustment stage, in which the interparticle macropores and mesopores were compressed. The content of interparticle macropores and mesopores decreased, while the interparticle micropores increased, suggesting that under axial strains of less than 8%, triaxial shearing compressed the interparticle macropores and mesopores into interparticle micropores.

During Stage II, the content of interparticle micropores continued to increase slowly, while the content of interparticle mesopores decreased. Compared with Stage I, the content of interparticle macropores changed little. In Stage II, the structure of the interparticle macropores gradually stabilized. Under the confining pressure of 400 kPa, the variation of all three pore types was smaller to that under confining pressures of 100 and 200 kPa. During axial shearing, the interparticle macropores were stable, while the interparticle micropores and mesopores continued to adjust. Once the axial strain reached 16%, the pores inside the soil sample stabilized, and the pore distribution remained unchanged as axial strain continued to increase.

During Stage III, the content of pores under low confining pressures (100 and 200 kPa) did not change. As axial strain increased, the interparticle macropores and mesopores were gradually compressed. The interparticle macropores content decreased gradually, and the content of interparticle micropores increased gradually. Under high confining pressure (400 kPa), the content of interparticle mesopores decreased, but the extent of this change was small. In contrast, the content of interparticle macropores increased. Under high confining pressure, once the axial strain reached 16%, the internal structure of the soil changed a second time, and tiny cracks began to form within the soil sample.

During triaxial shearing, the internal structure of the soil changed more quickly under higher confining pressure. When axial strain exceeded 8%, the pore changes of the soil stabilized after an initial adjustment of the internal pores of the soil. Under a confining pressure of 200 kPa or less, it took greater strain to complete this adjustment of the internal structure of the soil.

Conclusions

1. Under different confining pressures and axial strains, the pore content of the soil samples with pore diameters of less than 1 μm was almost constant, suggesting intragranular pores were not greatly affected by the test.

2. Under consolidation tests, the stress state of the soil sample changed, and the pores within the soil sample were rearranged. Typically, the interparticle macropores were initially compressed into interparticle mesopores, but as the confining pressure increased, the interparticle macropores and mesopores were compressed into interparticle micropores. The greater the confining pressure, the greater the compression effect on the interparticle mesopores and macropores.

3. During the triaxial tests, when axial strain was between 0% and 8%, the pore structure in the soil sample underwent a sharp adjustment stage, in which interparticle macropores and mesopores were compressed greatly. The pore number decreased rapidly, although interparticle micropores increased. Shearing compressed interparticle macropores and mesopores into interparticle micropores.

4. Increasing the confining pressure accelerated the adjustment of the pores during shearing. When the confining pressure was larger, a smaller axial strain facilitated adjustment of the interparticle pores of the soil.

Acknowledgements

This research supported by the National Natural Science Foundation of China (41762022, 41967037) and the Guilin Science and Technology Research and Development Project (20170222).

REFERENCES

1. J. Tchalenko and N. Morgenstern, "Microscopic structures in kaolin subjected to direct shear," *Geotechnique*, **17**, 309-328 (1967).
2. A. Casagrande, "The structure of clay and its importance in foundation engineering," *Boston Soc. Civ. Eng. J.*, **19**(4), 168-209 (1932).
3. P. Delage and G. Lefebvre, "Study of the structure of a sensitive Champlain clay and of its evolution during consolidation," *Can. Geotech. J.*, **21**(1), 21-35 (1984).
4. Y. Shan, H. Mo, S. Yu and J. Chen "Analysis of the maximum dynamic shear modulus and particle arrangement properties of saturated soft clay soils," *Soil Mech. Found. Eng.*, **53**(4): 226-232(2016).
5. E. Alonso, N. Pinyol, and A. Gens, "Compacted soil behaviour: initial state, structure and constitutive modelling," *Geotechnique*, **63**(6), 463-478 (2013).
6. B. T. Lin and A. B. Cerato, "Shear strength of shale weathered expansive soils along swell-shrink paths: analysis based on microscopic properties," *Environ. Earth Sci.*, **74**(9), 6887-6899 (2015).
7. G. L. Tao, W. Peng, H. L. Xiao, X. K. Wu, and Y. Chen, "Numerical simulation and microscopic stress mechanism for the microscopic pore deformation during soil compression," *Adv. Civ. Eng.*, **2019**(4), 1-14 (2019).
8. D. P. Gallegos and D. M. Smith, "A NMR technique for the analysis of pore structure: Determination of continuous pore size distributions," *J. Colloid Interface Sci.*, **122**(1), 143-153 (1988).
9. H. Daigle and A. Johnson, "Combining mercury intrusion and nuclear magnetic resonance measurements using percolation theory," *Transport Porous Med.*, **111**(3), 669-679 (2016).
10. F. Jaeger, S. Bowe, H. Van As, and G. Schaumann, "Evaluation of 1H NMR relaxometry for the assessment of pore-size distribution in soil samples," *Eur. J. Soil Sci.*, **60**(6), 1052-1064 (2009).
11. K. Zhou, Z. Hu, F. Gao, and M. Wang, "Study of marble damage laws under triaxial compression condition based on nuclear magnetic resonance technique," *Rock Soil Mech.*, **35**, 3117-3122 (2014).
12. Y. Liu, Z. Li, L. Guo, W. Kang, and Y. Zhou, "Pore characteristics of soft soil under triaxial shearing measured with NMR," *Rock Mech. Eng.*, **37**(08), 1924-1932 (2018).